# MRI After Treatment of Locally Advanced Rectal Cancer: How to Report Tumor Response—The MERCURY Experience

Uday B. Patel[1]
Lennart K. Blomqvist[2]
Fiona Taylor[3]
Christopher George[4]
Ashley Guthrie[5]
Nicola Bees[3]
Gina Brown[1]

**OBJECTIVE.** The Magnetic Resonance Imaging and Rectal Cancer European Equivalence (MERCURY) Study validated the use of MRI for posttreatment staging and its correlation with survival outcomes. As a consequence, reassessment of MRI scans after preoperative therapy has implications for surgical planning, the timing of surgery, sphincter preservation, deferral of surgery for good responders, and development of further preoperative treatments for radiologically identified poor responders.

**CONCLUSION.** In this article we report a validated systematic approach to the interpretation of MR images of patients with rectal cancer after chemoradiation.

**Keywords:** chemoradiation, MRI, rectal cancer, restaging

DOI:10.2214/AJR.11.8210

Received November 9, 2011; accepted after revision February 29, 2012.

The funding of the original MERCURY Study was provided by educational grants from Siemens Medical UK and the Pelican Cancer Foundation. U. B. Patel and G. Brown are supported by the NIHR Biomedical Research Center.

[1]Department of Radiology, Royal Marsden Hospital, Downs Rd, Sutton SM2 5PT, United Kingdom. Address correspondence to G. Brown (gina.brown@rmh.nhs.uk).

[2]Department of Radiology, Karolinska University Hospital, Solna, Stockholm, Sweden.

[3]Department of Radiology, Mayday University Hospital, Croydon, United Kingdom.

[4]Department of Radiology, Epsom General Hospital, Epsom, United Kingdom.

[5]Department of Radiology, St. James Hospital, Leeds, United Kingdom.

**WEB**
This is a Web exclusive article.

*AJR* 2012; 199:W486–W495

0361–803X/12/1994–W486



High-spatial-resolution MRI is already established as an accurate tool for the preoperative staging of rectal cancer [1] and has resulted in marked improvements in staging accuracy compared with historic studies [2]. MRI also defines the relationship between a tumor and the mesorectal fascia, which denotes the circumferential resection margin at total mesorectal excision. The potential circumferential resection margin is considered involved if tumor extends to within 1 mm of this fascia. Patients with locally advanced T3 or T4 disease or disease involving the potential circumferential resection margin on baseline MRI are offered chemoradiation therapy (CRT). This approach has been shown to decrease the postoperative tumor recurrence rate [3].

Until recently, the precise role, importance, and validity of restaging rectal cancers after preoperative therapy have been uncertain [4]. The Magnetic Resonance Imaging and Rectal Cancer European Equivalence (MERCURY) Study evaluated consecutive patients undergoing both primary surgery and preoperative therapy with histopathologic correlation and analyzed survival outcomes [5]. The results of the MERCURY Study showed that post-CRT MRI assessment of tumor regression grade correlated with disease-free survival and overall survival and, thus, with patient prognosis. Furthermore, posttreatment MRI prediction of potential circumferential resection margin involvement also gave prognostic information regarding the risk of local recurrence.

In this study both posttreatment MRI T staging and posttreatment MRI assessment of tumor regression grade showed statistical correlation with pathologic T stage, which in turn was strongly associated with overall and disease-free survival as well as local recurrence [5].

MRI's ability to identify good and poor responses after preoperative therapy enables further tailoring of treatment [6]. For example, a patient with MRI findings suggestive of a poor response or MRI findings showing persistence of a potentially involved circumferential resection margin could be offered systemic non–cross-resistant chemotherapy or a radical surgical exenterative procedure. Conversely, phase II trials are currently evaluating the safety of deferring surgical resection in patients with a good response as shown on MRI [7, 8].

Posttreatment MRI tumor regression grade and circumferential resection margin evaluation give the multidisciplinary team a valuable opportunity to further refine treatment plans according to the response seen on high-resolution MRI. This article focuses on how to report MRI findings after CRT of patients with rectal cancer and provides illustrated examples.

## MR Technique

Baseline T staging of rectal tumors using thin-slice MRI was first shown to accurately match pathologic T stage in 1999 [9]. The details of the MRI technique were published

in 2005 and its accurate reproducibility was confirmed in 2007 [10, 11]. This high-resolution technique is recommended for optimal visualization of rectal and mesorectal anatomy [12] and for characterization of mesorectal lymph nodes [13]. The same technique was used for posttreatment assessment in the MERCURY Study [5]; in that study, high-resolution T2-weighted images were found to be particularly useful in differentiating tumor from fibrosis. Comparison of posttreatment MR images with pretreatment MR images is essential and ideally both are acquired using the same angles. Pretreatment images are used to help locate the treated tumor, which may be difficult to visualize in patients who have had a good response to CRT. Our center does not use purgative bowel preparation or enemas [10]. The full MR parameters are detailed in Table 1.

After initial localization imaging, large-FOV sagittal and axial images are acquired [10]. These first two sequences allow an overview of the treated tumor, potentially involved lymph nodes, and direction of the rectal wall. This overview enables the planning of the following three high-spatial-resolution sequences that are vital for visualization of the tumor and posttreatment fibrosis.

The first sequence planned is axial to the plane of the tumor and rectal wall (Fig. 1A). Thin-section (maximum, 3 mm) axial T2-weighted images through the treated rectal cancer are planned using the sagittal T2-weighted images. These images are obtained perpendicular to the long axis of the rectum using a 16-cm FOV.

The second sequence is oblique axial imaging for evaluation of the lymph node drainage territory (Fig. 1B). Further oblique axial imaging to ensure coverage of the draining nodes and tumor deposits—which can extend above the superior edge of tumor—should be performed.

The third sequence is in the coronal plane for low rectal cancers (Fig. 1C).

Relying on oblique axial imaging alone can be limiting at the level of the anorectal junction. At that level, the rectal wall changes in diameter and the distance to the neighboring tissues is smaller. The images may not show the rectal wall in its entirety and overstaging may result from partial volume averaging. Therefore, high-resolution coronal imaging, which will show the relationship between the rectal wall and the levator muscles and between the anal sphincter complex and the intersphincteric plane, is useful for tumors in the lower one third of the rectum.

Overall this MRI protocol takes 30–40 minutes to perform in our center.

**TABLE 1: MRI Parameters for 1.5-T System [52][a]**

| Parameter | Fast Spin-Echo | |
|---|---|---|
| | Standard 3- to 5-mm Sagittal and Axial Images | High-Resolution Oblique Axial and Coronal Images[b] |
| TR (ms) | | |
| Sagittal | 5080 | |
| Axial | 4018 | 5362 |
| TE (ms) | | |
| Sagittal | 132 | 100 |
| Axial | 80 | |
| No. of slices | | |
| Sagittal | 23 | 16 |
| Axial | 20 | |
| Thickness and gap (mm) | | |
| Sagittal | 3 | 3 and 0.3 |
| Axial | 5 and 1 | |
| Interleaved | No | Yes |
| Echo-train length | 23 | 16 |
| Matrix | | |
| In phase direction | 512 | |
| In phase encoding | | 256 |
| Phase-encoding direction | Anteroposterior | Inferosuperior |
| FOV (mm) | 250 | 160 |
| Phase | 250 | |
| Frequency | 250 | |
| No. of acquisitions | | |
| Sagittal | 3 | 6 |
| Axial | 2 | |
| Flow compensation | Yes | No |
| Saturation bands | Anterior and superior | None |

[a]Parameters shown here are for a Philips Healthcare unit. Parameters for MR units manufactured by Siemens Healthcare and GE Healthcare are provided in reference [52].
[b]For tumors in the lower one third of the rectum.

## Additional MR Techniques

In radiology departments 3-T MR systems are increasingly available. These systems shorten the examination time because 3D image acquisitions remove the need for additional multiplanar 2D images [14]. Improved spatial resolution and signal-to-noise ratio have also been reported [14]. Studies comparing 2D and multiplanar reconstruction 3D T2-weighted imaging protocols in staging rectal cancer have shown no significant differences in T staging [15] and N staging [14, 16] accuracy. These studies did not investigate the accuracy of 3D T2-weighted imaging in restaging rectal cancer after CRT and our experience in this setting is also limited. In this article, we present images acquired using a 1.5-T whole-body MR imager with a pelvic phased-array coil.

Dynamic contrast-enhanced MRI (DCE-MRI) has also been evaluated in the restaging of rectal cancer after CRT. Devries et al. [17] ($n$ = 17) showed DCE-MRI perfusion index values before chemoradiation correlated with T downstaging. Dinter et al. [18] ($n$ = 33) showed the slope of the contrast medium enhancement curve helped to identify responders to CRT. Overall, in the absence of published evidence regarding the accuracy and reproducibility of DCE-MRI and DCE-MRI's comparative value versus high-resolution T2 scanning, we do not recommend DCE-MRI for routine use in restaging rectal cancer.

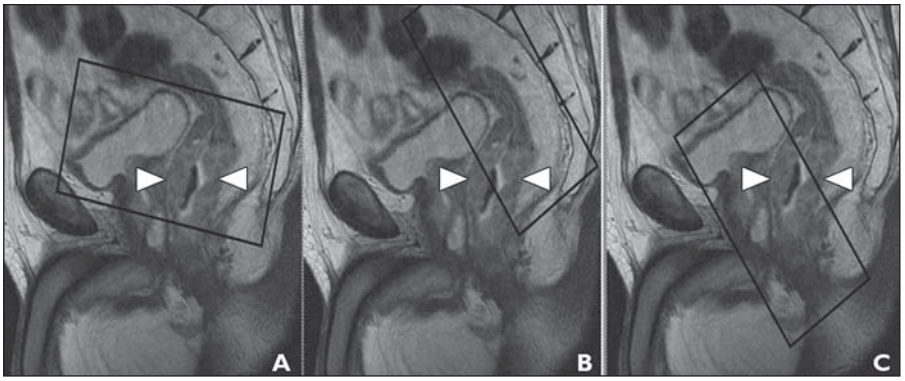


**Fig. 1**—70-year-old man with rectal cancer.
**A,** Planned high-resolution block (*box*) axial to plane of tumor and rectal wall. Images are acquired perpendicular to long-axis of rectum. Tumor is indicated by arrowheads.
**B,** Oblique axial block (*box*) to cover lymph node drainage territory. Lymph nodes can extend above superior edge of tumor. Tumor is indicated by arrowheads.
**C,** Block in coronal plane (*box*) for imaging tumors in low one third of rectum. This image shows relationship between rectal wall and levator muscles and between anal sphincter complex and intersphincteric plane. Tumor is indicated by arrowheads.

We recommend that the following parameters are assessed on posttreatment MR images:

- Morphologic appearance of tumor including any mucinous or necrotic component;
- Height of treated tumor from the anal verge compared with that on baseline pretreatment scans;
- Length of tumor compared with length on baseline pretreatment scans;
- MRI tumor regression grade;
- Depth of maximum extramural spread (i.e., distance from outermost edge of muscularis propria) of tumor and fibrosis given separately;
- MRI T stage and T substage of tumor, taking into account depth of extramural spread;
- Distance to potential circumferential margin and whether this area appears involved or clear;
- Extramural venous invasion;
- Lymph node staging including whether nodes in the pelvic sidewall compartment are involved; and
- Potential involvement of the peritoneal reflection.

## Morphologic Responses

Morphologic changes seen in surgical specimens after CRT include collagen, fibrosis, desmoplasia, mucin, inflammatory change resulting in submucosal edema, and necrosis. The next sections correlate these pathologic changes with appearances on posttreatment MRI.

### *Fibrotic Changes to Tumor and the Rectal Wall*

Pathologically, fibrotic stroma consists of matrix components such as collagen as well as cells responsible for matrix production such as fibroblasts and histiocytes [19]. Fine and elongated collagen fibers stratified into layers make up mature fibrotic stroma, whereas immature fibrotic stroma consists of randomly oriented collagen bundles [20].

On post-CRT T2-weighted MRI, we found that areas of fibrosis have very low signal intensity, whereas areas of residual tumor have intermediate signal-intensity. The signal intensity of fibrosis is similar to that of the muscularis propria, and signal intensity of residual tumor is similar to that of baseline tumor. Careful review of high-resolution images will enable delineation of small foci of intermediate-signal-intensity tumor within areas of low-signal-intensity fibrosis. Figure 2 shows an example of tumor regression within the rectal wall leaving a fibrotic low-signal-intensity scar while a focus of intermediate-signal-intensityresidual disease remains in a vein.

### *Desmoplastic Reaction*

Desmoplastic reaction is also called "reactive fibrosis." Pathologically this process in-

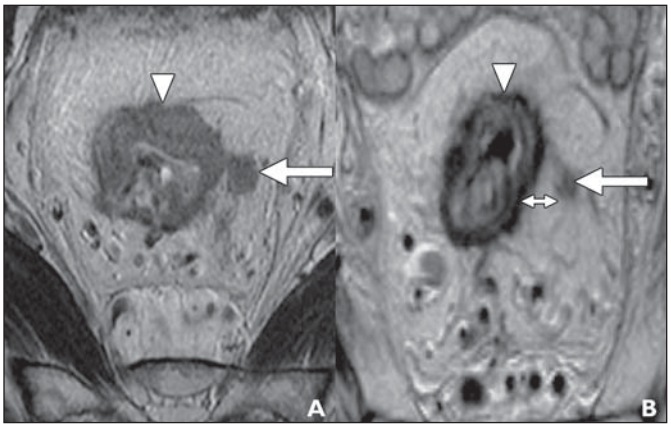


**Fig. 2**—67-year-old man with rectal cancer.
**A,** Baseline axial T2-weighted MR image shows semiannular infiltrating tumor (*arrowhead*). Nodule (*arrow*) of intermediate signal intensity is seen in medium-sized vein at 3-o'clock position.
**B,** Posttreatment axial image shows tumor regression within rectal wall. Fibrotic low-signal-intensity scar (*arrowhead*) is seen between 9- and 4-o'clock positions. Focus of residual disease (*single-headed arrow*) remains in vein at 3-o'clock position. Overall these MR findings show mixed response to treatment; MRI assessment of tumor regression grade is 3. Residual venous disease is 6 mm (*double-headed arrow*) beyond muscularis propria indicating posttreatment T3c stage.

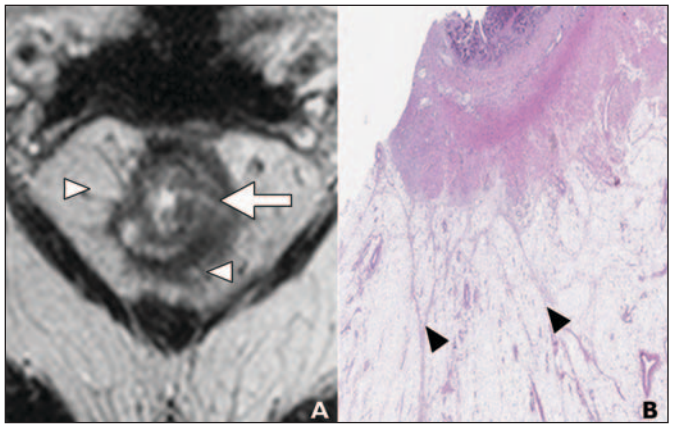


**Fig. 3**—65-year-old woman with rectal cancer.
**A,** Posttreatment axial T2-weighted image shows semiannular tumor (*arrow*) between 12- and 4-o'clock positions. Low-intensity spicules in perirectal fat radiating from residual tumor (*arrowheads*) represent desmoplastic reaction.
**B,** Corresponding photomicrograph (H and E, ×0.4) shows desmoplastic reaction (*arrowheads*).

volves the deposition of collagen as a stromal response. Anatomic distortion can be caused as a result. Desmoplastic reaction does not contain tumor.

On baseline and post-CRT MRI, this reaction is seen as low-intensity spicules or strands in the perirectal fat radiating from the residual tumor. Figures 3A and 3B illustrate desmoplastic reaction.

Misinterpretation of desmoplastic reaction for residual tumor can lead to overstaging because the spiculated areas are presumed to represent tumor rather than reaction. In our experience an advancing tumor margin has a more nodular, intermediate-signal-intensity appearance; Figures 4A and 4B illustrate this appearance [9].

### *Mucinous Change in Tumors*

Mucin formation occurs in the following three scenarios.

*The first scenario*—Pathologic studies describing posttherapeutic changes have noted mucinous response in nonmucinous tumors. This response has been shown to be of prognostic significance and in keeping with a treatment response effect [21]. On baseline imaging, a nonmucinous tumor corresponds to a tumor that is of entirely intermediate signal intensity with no areas of high-signal-intensity mucin. After CRT, necrosis of the tumor can result in mucinous degeneration. In such cases, degeneration of the tumor results in high-signal-intensity pools within the previously documented intermediate-signal-intensity tumor stroma and can therefore be interpreted as evidence of treatment response.

*The second scenario*—Pathologically, mucinous rectal tumors comprise pools or lakes of extracellular mucin lined by columns of malignant cells, cords, and vessels. This composition gives an overall meshlike internal structure [21]. A recent analysis of 108 prospectively collected posttreatment specimens showed acellular mucin pools in 16 cases. The presence of acellular mucin pools had no impact on recurrence-free survival [22]. Therefore, acellular mucin is regarded as a type of treatment response and not as residual tumor [23].

Cellular mucin on T2 imaging is hyperintense [24] but contains more areas of intermediate signal intensity corresponding to the histologically shown malignant cells, cords, and vessels. After treatment, the necrosis of these viable nests and cords of tumor results in the formation of acellular mucin—namely, pools of featureless high-signal-intensity fluidlike signal on T2-weighted images that contain no or minimal intermediate signal intensity when compared with pretreatment scans (Figs. 5A and 5B).

*The third scenario*—Nonresponse is associated with poor outcomes; in mucinous tumors, nonresponse is reflected pathologically as persistent columns of malignant cells and cords. On MRI, tumors containing high signal with intermediate-signal-intensity components at baseline that are unchanged on posttreatment imaging indicate nonresponse. These tumors carry a poorer prognosis and increased risk of local recurrence [25]. Documentation of the extent of residual cellular mucin is important because the risk of tumor spillage from mucin pools will increase the risk of local recurrence.

### *Pseudotumor*

Rectal carcinoma often grows circumferentially and eventually can lead to annular stenosis of the bowel wall. The tumor often has central indentation with rolled everted edges and invasion or ulceration at its posterior border. The remaining rectal luminal mucosa and submucosa often appear heaped up into the lumen—a pseudotumor appearance (Fig. 6). This effect can get exaggerated after treatment response because the original tumor becomes fibrotic, low in signal intensity, and less bulky. These changes may result in near-normal thickness of treated rectal wall but the unaffected submucosa can become edematous, thickened, and of intermediate intensity, leading to potentially false interpretation.

This pitfall can be avoided by direct comparison of the pretreatment scans with the posttreatment scans and documentation of the invasive and rolled edge of tumor as well as the portion of the rectal wall circumference that has not been involved by tumor. Other signs such as desmoplastic reaction from the tumor are also helpful.

## MRI Assessments of Tumor Length and Modified Response Evaluation Criteria in Solid Tumors

The change in maximum tumor length between baseline and posttreatment sagittal images has been investigated as a tool to evaluate tumor response [26, 27]. The percentage change in tumor length has been classified using the Response Evaluation Criteria in Solid Tumors (RECIST), with complete disappearance of tumor being defined as complete re-

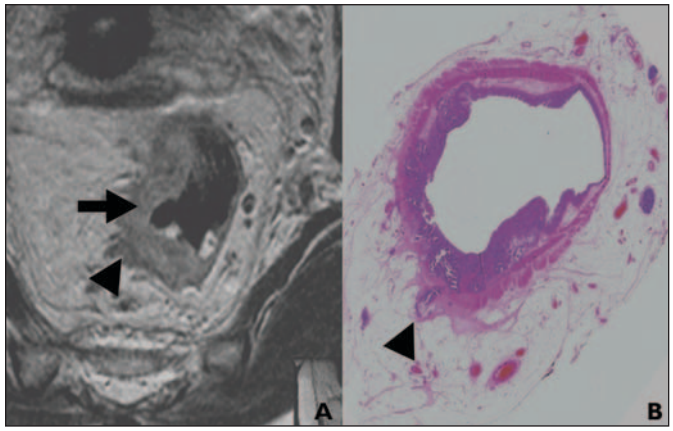


**Fig. 4**—63-year-old woman with rectal cancer.
**A,** Posttreatment axial T2-weighted image shows semiannular tumor (*arrow*). Intermediate-signal-intensity nodule (*arrowhead*) advancing into mesorectal fat is seen; this finding is consistent with tumor infiltration.
**B,** Corresponding photomicrograph (H and E, ×0.4) shows nodular tumor infiltration (*arrowhead*) into mesorectal fat.

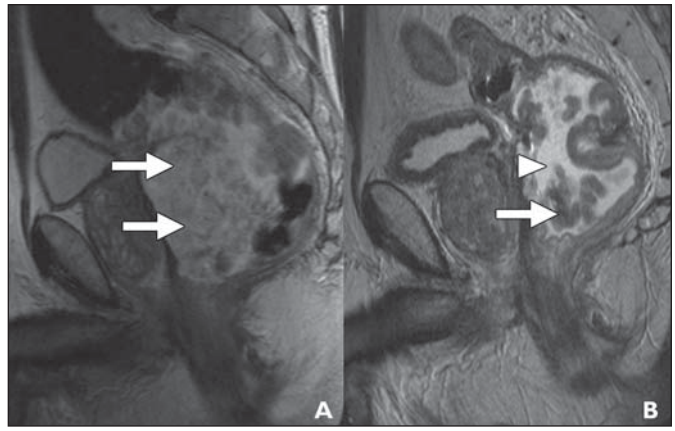


**Fig. 5**—80-year-old man with rectal cancer.
**A,** Baseline sagittal T2-weighted image shows large tumor with high signal intensity compatible with mucin. Intermediate-signal-intensity solid cellular components (*arrows*) are noted within tumor.
**B,** Posttreatment sagittal T2-weighted image shows acellular mucin, indicated by featureless areas of high signal intensity (*arrowhead*), has formed since **A**. Areas of intermediate-signal-intensity residual tumor (*arrow*) remain.

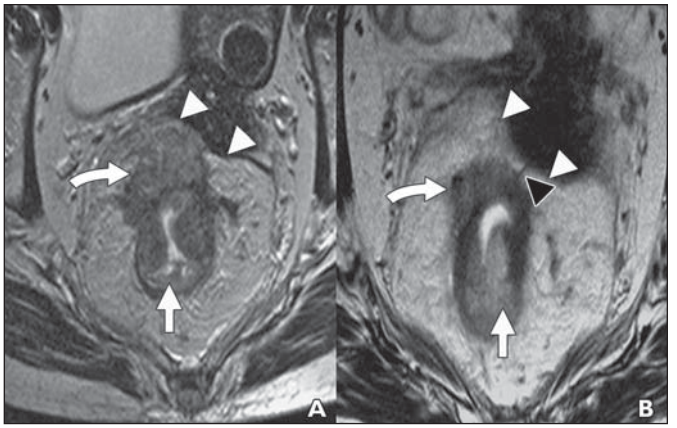


**Fig. 6**—70-year-old woman with rectal cancer.
**A,** Axial T2-weighted MR image shows semiannular tumor (*curved arrow*). Unaffected portion of rectal wall (*straight arrow*) is in posterior midline. Circumferential resection margin (*arrowheads*) is potentially involved because tumor infiltrates to within 1 mm of it.
**B,** MR image obtained after chemoradiation therapy shows tumor (*curved arrow*) is at 12-o'clock position and pseudotumor (*straight arrow*), due to treatment-related edema of mucosa and submucosa, is at 6-o'clock position. Linear low-signal-intensity strands of desmoplastic reaction (*black arrowhead*) extend toward circumferential resection margin (*white arrowheads*).

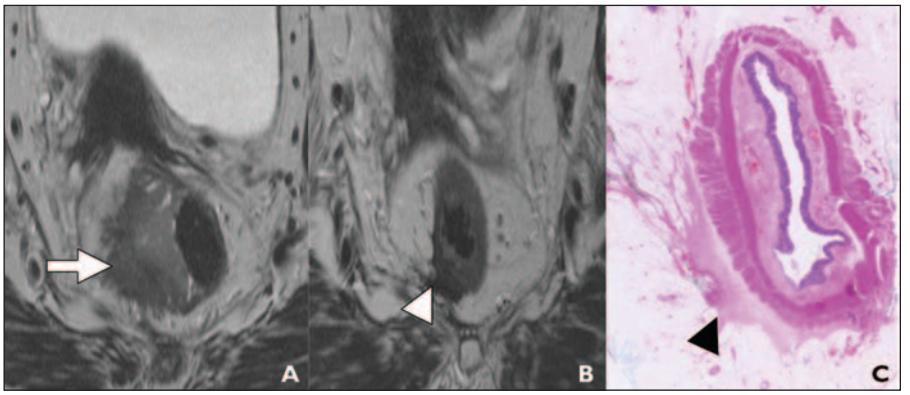


**Fig. 7**—69-year-old woman with rectal cancer.
**A,** Baseline axial T2-weighted MR image shows semiannular infiltrating tumor (*arrow*).
**B,** Posttreatment axial image shows fibrotic low-signal-intensity scar (*arrowhead*) at 7- to 8-o'clock position. Absence of tumor signal indicates MRI assessment of tumor regression grade is 1.
**C,** Photomicrograph (H and E, ×0.4) shows fibrosis (*arrowhead*) extends beyond muscularis propria.

sponse. Partial response to treatment is defined as at least a 30% decrease in tumor length. Progression of disease is defined as at least a 20% increase in tumor length, and stable disease is defined as neither sufficient shrinkage to qualify for partial response nor sufficient increase to qualify for progression of disease [28].

This approach has been investigated in two clinical trials. The EXPERT-C Trial (mulicenter randomized phase 2 clinical trial comparing oxaliplatin, capecitabine, and preoperative radiotherapy with or without cetuximab followed by total mesorectal excision) has shown good correlation between RECIST assessment and survival outcomes [29]. However, the CORE (capecitabine, oxaliplatine, radiotherapy, and excision) Trial showed that the reproducibility of tumor length between two readers was only slight ($\kappa = 0.13$) despite good correlation between length assessment and histopathologic T stage [30]. Therefore, length measurements are useful in the assessment of tumor response but may need to be undertaken by central review in clinical trials because of the lack of interobserver reproducibility.

## Pathologic Tumor Regression Grading

Dworak et al. [31] reviewed 17 surgical specimens after CRT and described varying degrees of replacement of tumor with fibrous or fibroinflammatory tissue. The degree of fibrosis versus the degree of residual tumor is used as the basis for the Dworak tumor regression grading system [31] as well as the modified Mandard tumor regression system [32]. These systems provide information about the grade of tumor regression and response to CRT that is not readily available from T staging.

Validation of pathologic tumor regression grading was undertaken by Rödel et al. [33] in 385 patients treated with CRT. Their results showed that patients with complete and those with partial pathologic tumor regression had improved disease-free survival compared with patients with minimal pathologic tumor regression. Applying similar principles with

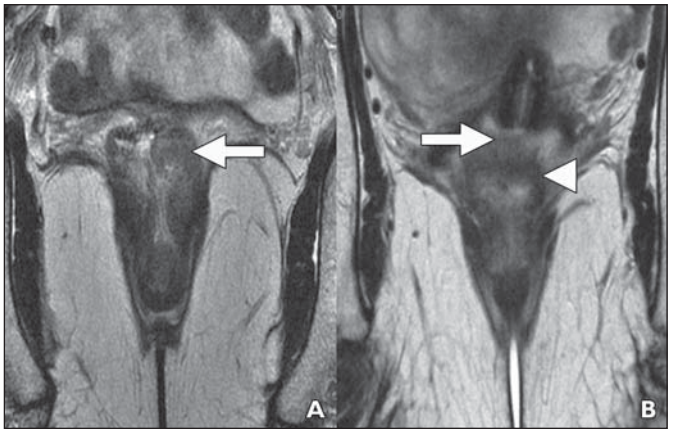


**Fig. 8**—31-year-old woman with rectal cancer.
**A,** Baseline coronal T2-weighted image shows semiannular tumor (*arrow*) between 12- and 5-o'clock positions.
**B,** Posttreatment coronal T2-weighted image shows tumor regression within rectal wall and fibrotic low-signal-intensity scar (*arrowhead*). Small amount of residual intermediate signal intensity (*arrow*) indicating tumor is noted. Overall these findings are compatible with MRI tumor regression grade of 2.

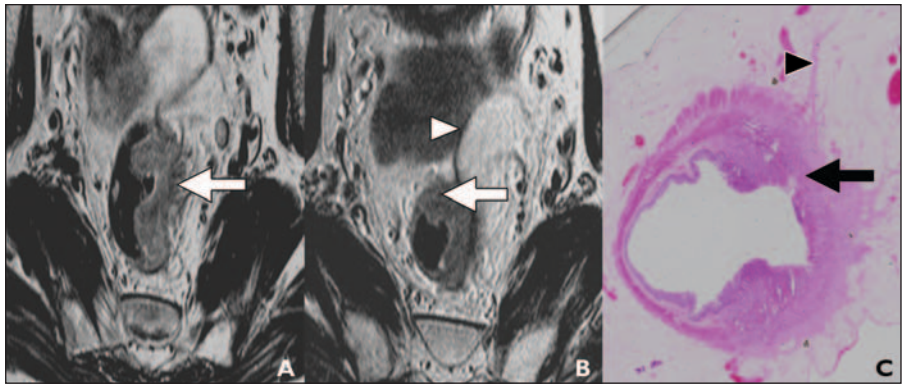


**Fig. 9**—60-year-old man with rectal cancer.
**A,** Baseline axial T2-weighted MR image shows semiannular infiltrating tumor (*arrow*) between 1- and 5-o'clock positions.
**B,** Posttreatment axial image shows fibrotic low-signal-intensity extramural rim (*arrowhead*); however, dominant residual intermediate-signal-intensity tumor (*arrow*) is present. Overall these MR findings are consistent with MRI assessment of tumor regression grade of 4.
**C,** Photomicrograph (H and E, ×0.4) shows extramural fibrosis (*arrowhead*) with residual tumor (*arrow*) between 1- and 5-o'clock positions.

**TABLE 2: Survival Outcomes of 111 Patients Who Underwent Preoperative Therapy in the Magnetic Resonance Imaging and Rectal Cancer European Equivalence (MERCURY) Study**

| Posttreatment MRI | Frequency (No. of Patients) | Overall Survival (95% CI) | Disease-Free 5-Year Survival (95% CI) | Local Recurrence (95% CI) |
|---|---|---|---|---|
| Tumor regression grade | | | | |
| Grades 1–3 (good) | 32 | 72 (56–88)[a] | 64 (47–82)[b] | 14 (1–27) |
| Grades 4 and 5 (poor) | 34 | 27 (8–47)[a] | 31 (13–49)[b] | 29 (8–49) |
| Missing | 45 | | | |
| Potential circumferential resection margin involvement[d] | | | | |
| Margin clear | 64 | 59 (46–71) | 58 (46–71) | 12 (3–22)[c] |
| Posttreatment | 55 | | | |
| Baseline only | 9[e] | | | |
| Margin involved | 47 | 46 (31–61) | 51 (35–67) | 28 (13–44)[c] |
| Posttreatment | 37 | | | |
| Baseline only | 10[f] | | | |
| No posttreatment MRI | 19 | | | |
| N stage | | | | |
| N0 | 50 | 61 (47–76) | 63 (49–78)[g] | 18 (5–33) |
| N1 and N2 | 40 | 45 (29–61) | 46 (29–63)[g] | 17 (3–32) |
| Missing | 21 | | | |
| T stage | | | | |
| T0 | 6 | 73 (54–92) | 72 (52–91) | 20 (2–38) |
| T1 and T2 | 13 | | | |
| T3a | 4 | | | |
| T3b | 14 | 48 (35–60) | 50 (37–64) | 16 (6–27) |
| T3c | 22 | | | |
| T3d | 9 | | | |
| T4 | 22 | | | |
| No posttreatment MRI | 21 | | | |

[a] $p = 0.001$.
[b] $p = 0.007$.
[c] $p = 0.013$.
[d] When posttreatment scanning was not performed, the circumferential resection margin at baseline was entered as the circumferential resection margin status.
[e] Nine of nine showed clear pathologic circumferential resection margin involvement.
[f] Five of 10 had pathologic circumferential resection margin involvement.
[g] $p = 0.027$.

MRI, we have now shown that it is possible to assess tumor regression before surgery.

### MRI Tumor Regression Grading

With data from the MERCURY Study [5], an MRI-based tumor regression grading system was developed reflecting the equivalent definitions used for the Dworak tumor regression grading system. The entire tumor is assessed to determine if fibrous signal intensity or if tumor signal intensity predominates [34]. The radiologic interpretation requires comparison of high-resolution oblique images with baseline scans to determine the proportion of tumor that has become of fibrotic low signal intensity and the proportion of remaining residual intermediate signal intensity. If there is a predominance of fibrosis with no or minimal residual intermediate tumor signal, a tumor regression grade of 1 or 2, respectively, is assigned as illustrated in Figures 7 and 8. If there is substantial tumor signal-intensity present but that signal-intensity does not predominate the fibrosis, a tumor regression grade of 3 is assigned (Fig. 2). If there is a predominance of tumor with minimal low-signal-intensity fibrosis, a tumor regression grade of 4 is assigned (Fig. 9). If the tumor appears unchanged from baseline, the tumor regression grade is 5.

In the MERCURY Study [5], patients treated with CRT who underwent posttreatment MRI were retrospectively independently assessed for MRI tumor regression grade. MRI assessment of tumor regression grade was a significant independent predictor of overall survival and disease-free survival. These results are shown in Table 2.

### T Staging After Chemoradiation Therapy

Interpretation of T stage after CRT requires careful delineation of the relationship of any persistent tumor signal intensity to the rectal wall. High-resolution scans are essential to enable accurate distinction of residual tumor signal intensity versus fibrosis signal intensity and to depict the area of treated tumor.

The T staging categories [35] are the same as baseline staging criteria (Table 3). As with pretreatment staging, it is important to recognize that tumor spread of less than 1 mm beyond

**TABLE 3: T Staging of Rectal Tumors on MRI [35]**

| T Stage | Description |
|---|---|
| Tx | Primary tumor cannot be evaluated |
| T0 | No evidence of primary tumor |
| T1 | Invasion of submucosa by tumor; abnormal signal-intensity has replaced submucosa |
| T2 | Invasion but not penetration of muscularis propria; intermediate signal intensity in muscularis propria |
| T3 | Invasion of subserosa through muscularis propria; broad bulge or nodular projection of intermediate signal-intensity extending beyond muscularis propria |
| 3a | < 1 mm beyond the muscularis propria |
| 3b | 1–5 mm beyond the muscularis propria |
| 3c | > 5 and ≤ 15 mm beyond the muscularis propria |
| 3d | > 15 mm beyond the muscularis propria |
| T4 | Invasion of other organs |
| T4a | Abnormal signal intensity extends into adjacent organs through peritoneal reflection |
| T4b | Tumor invades visceral peritoneum |

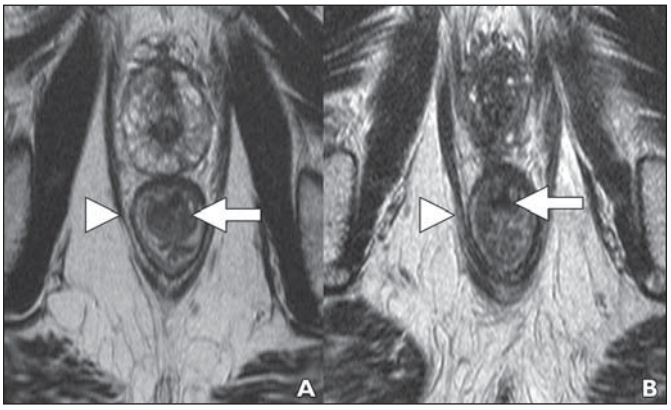


**Fig. 10**—68-year-old man with rectal cancer.
**A,** Baseline axial T2-weighted MR image at level of puborectalis (*arrowhead*) shows T1 tumor (*arrow*). Tumor is predominantly intramural with likely invasion of submucosa.
**B,** Posttreatment axial T2-weighted MR image obtained shows low-signal-intensity scar (*arrow*) at 12-o'clock position and normal submucosa. Puborectalis sling is indicated by arrowhead.

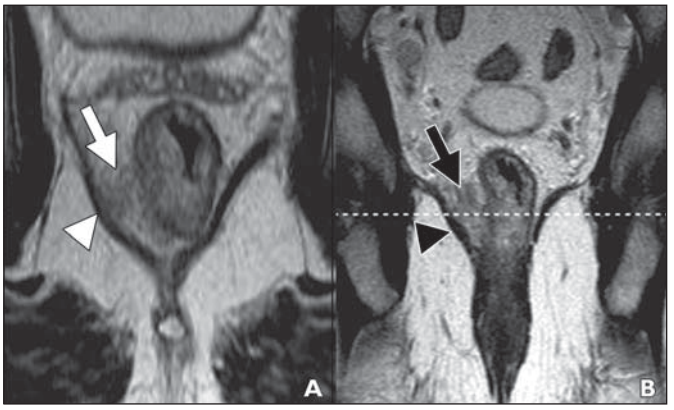


**Fig. 11**—80-year-old man with rectal cancer.
**A,** Baseline axial T2-weighted MR image shows semiannular infiltrating tumor (*arrow*) between 7- and 9-o'clock positions. Tumor extends extramurally and is less than 1 mm from left levator muscle (*arrowhead*). Potential resection margin is therefore threatened.
**B,** Baseline coronal T2-weighted MR image shows extramural tumor extension (*arrow*) up to left levator muscle (*arrowhead*). Dashed line indicates localiser.

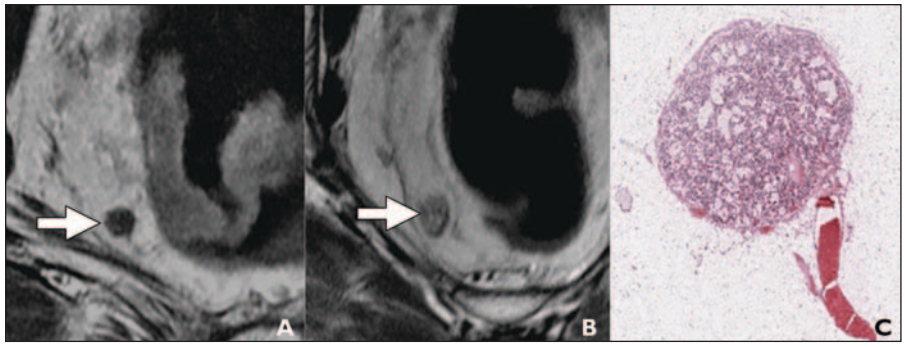


**Fig. 12**—65-year-old woman with rectal cancer.
**A,** Axial T2-weighted MR image shows lymph node (*arrow*) in right lower mesorectum. Malignancy is indicated by irregular edge and signal inhomogeneity.
**B,** Image obtained after chemoradiotherapy shows that node (*arrow*) continues to have irregular edge and that signal inhomogeneity persists; these findings indicate malignancy.
**C,** Corresponding photomicrograph (H and E, ×0.7) shows widespread tumor deposition in lymph node with irregular border. Because there is minimal normal nodal tissue, lymph node is indistinguishable from extranodal deposit.

the muscularis propria can be considered to be prognostically identical to T2 tumors; therefore, the differentiation of T2 from borderline T3 spread is not of clinical relevance [5].

The extent of fibrosis should be documented and recorded as an entity separate from the extent of tumor signal because fibrosis may or may not contain viable tumor and may be managed differently. Figure 2 illustrates an example of residual tumor and fibrosis at differing extramural depths.

Using these guidelines to restage rectal tumors has shown good correlation between posttreatment MRI T stage and histopathology. For example, in a prospective phase II trial for MRI-defined locally advanced rectal cancer, posttreatment MRI T stages T3b–T4 (35/43) were significantly associated with an unfavorable pathologic T stage, compared with posttreatment MRI T stages of T0–T3a (6/30) ($p = 0.001$) [30].

## Potential Circumferential Resection Margin and Distal Resection Margin Involvement

The potential circumferential resection margin is considered involved on MRI if the shortest distance from the outermost part of the tumor to the adjacent mesorectal fascia is less than 1 mm [36]. The circumferential resection margin forms the plane of total mesorectal excision surgery, and this plane is defined by the mesorectal fascia at and above the level of the top of the puborectalis sling. Figure 6 shows an example of a potentially involved circumferential resection margin.

Below the puborectalis sling, the total mesorectal excision plane is defined as the space between the muscle coat of the rectum becoming the internal sphincter and the fibers of the puborectalis sling that merge with the external sphincter fibers. At this level, tumor invading the intersphincteric plane (Fig. 10) or extending to within 1 mm of the levator muscle is considered to potentially involve the circumferential resection margin (Fig. 11).

In recent studies, the MERCURY Study Group investigators validated the restaging accuracy of MRI in determining the risk of intersphincteric plane invasion by tumor and consequent pathologic margin involvement [37–39]. Although no direct comparison was made with endoluminal ultrasound or endoanal MRI techniques, the high spatial resolution afforded by improved pelvic phased-array surface coils has largely eliminated the need to assess tumors with endoluminal techniques. Furthermore, endoluminal ultrasound has not been recommended [40] in reassessing sphincter invasion after CRT because the technique cannot distinguish between tumor and fibrosis [41, 42].

Tumor reduces in both the axial and longitudinal planes. In the axial plane, a tumor that on baseline imaging is beyond the potential circumferential resection margin may regress to within the potential circumferential resection margin after CRT. Such patients are good candidates for total mesorectal excision because tumor is not likely to be beyond the fibrotic extent of disease. The results of the MERCURY Study [1] showed that after CRT the specificity of MRI for the prediction of a negative margin was 92%.

Post-CRT MR images may also show fibrotic low signal intensity within 1 mm of the potential circumferential resection margin. It is currently advocated that any surgery should remove fibrotic stroma regardless of whether residual tumor signal-intensity can be seen.

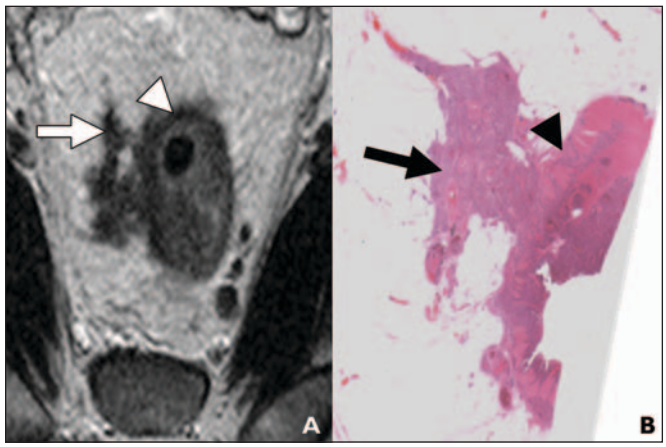


**Fig. 13**—60-year-old man with rectal cancer.
**A,** Axial T2-weighted MR image shows intermediate-signal-intensity tumor extending into neighboring vessel. Vessel (*arrow*) is expanded and irregular in contour. Bowel wall is shown by arrowhead.
**B,** Corresponding photomicrograph (H and E, ×0.7) shows tumor deposition (*arrow*) in vessel with irregular expansion. Bowel wall is indicated by arrowhead.

## Nodal Staging After Chemoradiation Therapy

CRT often reduces the size and number of benign and malignant lymph nodes. Frequently nodal downstaging is accompanied by tumor downstaging, whereas malignant nodes are often identified in those with significant residual disease.

Characterization of a node as benign or malignant uses morphologic rather than size criteria: A malignant node shows irregular outlines or internal signal heterogeneity, as shown in Figure 12. High-signal-intensity acellular mucinous denegation can also occur within lymph nodes and is a sign of treatment response [43]. Using these criteria, Koh et al. [43] showed MRI has an 80% positive predictive value, 90% negative predictive value, and 88% accuracy in detecting nodal disease after neoadjuvant treatment.

In the MERCURY Study [5], patients with nodal disease detected on posttreatment MRI had a disease-free 5-year survival rate of 46% compared with 63% for those with no

malignant nodes on posttreatment MRI ($p$ = 0.027) (Table 2).

### Extramural Venous Invasion After Treatment

Extramural venous invasion has been shown in 10–22% of postoperative specimens in colorectal cancer [44, 45]. Extramural venous invasion is defined by the presence of malignant cells within an endothelial cell–lined space that either is surrounded by a rim of smooth muscle or contains RBCs [46]. The degree of pathologic vascular invasion influences the likelihood of nodal dissemination [45], likelihood of liver metastasis, and survival rates [44].

The morphologic features of extramural venous invasion on baseline T2-weighted MRI range from discrete serpiginous or tubular projections of intermediate signal intensity into perirectal fat following the course of a visible vessel to, in more advanced cases, the vessel being expanded by intermediate-signal-intensity tumor and having an irregular contour [47, 48] (Fig. 13). The degree of extramural venous invasion system predicts relapse-free survival, with a 3-year relapse-free survival rate of 35% for patients with advanced extramural venous invasion, compared with 74% for those with no or early extramural venous invasion [48]. In our experience, extramural venous invasion can entirely disappear with treatment; fibrotic cords or strands signify a good response to treatment.

### Peritoneal Reflection Involvement

The typical appearance of peritoneal reflection involvement on baseline MRI is one of nodular intermediate signal intensity extending into the fine low-signal-intensity peritoneal reflection at or above the level of its attachment to the anterior surface of the rectum: This finding is best shown on sagittal and axial high-resolution images [49]. Such tumors are staged as T4a. Peritoneal reflection involvement is not readily identifiable by endoluminal ultrasound, and therefore peritoneal infiltration will not be detected by this method.

Currently there is a lack of randomized clinical trial data about the effect of preoperative therapy on peritoneal infiltration [50]. However, this may change in the future when the results of an ongoing clinical trial investigating preoperative treatment to tumors at and above the peritoneal reflection are fully reported [51]. Preoperative treatment of rectal cancer appeared to show a survival benefit in a retrospective study [50]. In that study, investigators found that 18 of 75 patients with upper rectal, rectosigmoid, or distal sigmoid tumors had T4 tumors invading adjacent organs (3/18) or had potentially circumferential resection margin involvement (15/18). These groups were offered preoperative CRT with significant pathologic tumor regression and fibrosis reported. Of the 18 patients offered CRT, two had positive histopathologic margins and the number of International Union Against Cancer stage III tumors was reduced from 16 (89%) to seven (39%) [50].

### Conclusion

Emerging evidence has shown the prognostic importance of reassessing rectal cancers using high-resolution T2-weighted MRI after completion of CRT. A systematic review of the known prognostic and morphologic features is essential for optimal treatment planning and patient care.

### References


1. MERCURY Study Group. Diagnostic accuracy of preoperative magnetic resonance imaging in predicting curative resection of rectal cancer: prospective observational study. *BMJ* 2006; 333:779
2. Bipat S, Glas AS, Slors FJ, Zwinderman AH, Bossuyt PM, Stoker J. Rectal cancer: local staging and assessment of lymph node involvement with endoluminal US, CT, and MR imaging—a meta-analysis. *Radiology* 2004; 232:773–783
3. Sauer R, Becker H, Hohenberger W, et al. Preoperative versus postoperative chemoradiotherapy for rectal cancer. *N Engl J Med* 2004; 351:1731–1740
4. Kim DJ, Kim JH, Lim JS, et al. Restaging of rectal cancer with MR imaging after concurrent chemotherapy and radiation therapy. *RadioGraphics* 2010; 30:503–516
5. Patel UB, Taylor F, Blomqvist L, et al. Magnetic resonance imaging–detected tumor response for locally advanced rectal cancer predicts survival outcomes: MERCURY experience. *J Clin Oncol* 2011; 29:3753–3760
6. O'Neill BD, Brown G, Heald RJ, Cunningham D, Tait DM. Non-operative treatment after neoadjuvant chemoradiotherapy for rectal cancer. *Lancet Oncol* 2007; 8:625–633
7. Yu SK, Brown G, Heald RJ, et al. Deferral of rectal surgery following a continued response to preoperative chemoradiotherapy (watch and wait) study: a phase II multicenter study in the United Kingdom (abstr). *J Clin Oncol* 2011; 29(suppl 4):abstract 489
8. Habr-Gama A, Perez RO, Nadalin W, et al. Operative versus nonoperative treatment for stage 0 distal rectal cancer following chemoradiation therapy: long-term results. *Ann Surg Oncol* 2004; 240:711–717; discussion, 717–718
9. Brown G, Richards CJ, Newcombe RG, et al. Rectal carcinoma: thin-section MR imaging for staging in 28 patients. *Radiology* 1999; 211:215–222
10. Brown G. Thin section MRI in multidisciplinary pre-operative decision making for patients with rectal cancer. *Br J Radiol* 2005; 78(Spec No 2):S117–S127
11. Koh DM, Brown G, Meer Z, Norman AR, Husband JE. Diagnostic accuracy of rim and segmental MRI enhancement of colorectal hepatic metastasis after administration of mangafodipir trisodium. *AJR* 2007; 188:502; [web]W154–W161
12. Koh DM, Brown G, Temple L, et al. Rectal cancer: mesorectal lymph nodes at MR imaging with USPIO versus histopathologic findings—initial observations. *Radiology* 2004; 231:91–99
13. Brown G, Richards CJ, Bourne MW, et al. Morphologic predictors of lymph node status in rectal cancer with use of high-spatial-resolution MR imaging with histopathologic comparison. *Radiology* 2003; 227:371–377
14. Kim H, Lim JS, Choi JY, et al. Rectal cancer: comparison of accuracy of local-regional staging with two- and three-dimensional preoperative 3-T MR imaging. *Radiology* 2010; 254:485–492
15. Maas M, Lambregts DM, Lahaye MJ, et al. T-staging of rectal cancer: accuracy of 3.0 Tesla MRI compared with 1.5 Tesla. *Abdom Imaging* 2012; 37:475–481
16. Fütterer JJ, Yakar D, Strijk SP, Barentsz JO. Preoperative 3T MR imaging of rectal cancer: local staging accuracy using a two-dimensional and three-dimensional T2-weighted turbo spin echo sequence. *Eur J Radiol* 2008; 65:66–71
17. Devries AF, Griebel J, Kremser C, et al. Tumor microcirculation evaluated by dynamic magnetic resonance imaging predicts therapy outcome for primary rectal carcinoma. *Cancer Res* 2001; 61:2513–2516
18. Dinter DJ, Horisberger K, Zechmann C, et al. Can dynamic MR imaging predict response in patients with rectal cancer undergoing cetuximab-based neoadjuvant chemoradiation? *Onkologie* 2009; 32:86–93
19. Knutsen A, Adell G, Sun XF. Inflammatory infiltration, fibrosis, necrosis and mucinous content in relation to clinicopathological and molecular factors in rectal cancers with or without preoperative radiotherapy. *Oncol Rep* 2006; 16:321–327
20. Ueno H, Jones AM, Wilkinson KH, Jass JR, Talbot IC. Histological categorisation of fibrotic cancer stroma in advanced rectal cancer. *Gut* 2004; 53:581–586
21. Rullier A, Laurent C, Vendrely V, Le Bail B, Bioulac-Sage P, Rullier E. Impact of colloid response on survival after preoperative radiotherapy in locally advanced rectal carcinoma. *Am J Surg Pathol* 2005; 29:602–606
22. Shia J, McManus M, Guillem JG, et al. Signifi-

cance of acellular mucin pools in rectal carcinoma after neoadjuvant chemoradiotherapy. *Am J Surg Pathol* 2011; 35:127–134

23. Compton CC. Key issues in reporting common cancer specimens: problems in pathologic staging of colon cancer. *Arch Pathol Lab Med* 2006; 130:318–324
24. Hussain SM, Outwater EK, Siegelman ES. Mucinous versus nonmucinous rectal carcinomas: differentiation with MR imaging. *Radiology* 1999; 213:79–85
25. Nagtegaal I, Gaspar C, Marijnen C, Van De Velde C, Fodde R, Van Krieken H. Morphological changes in tumour type after radiotherapy are accompanied by changes in gene expression profile but not in clinical behaviour. *J Pathol* 2004; 204:183–192
26. Torkzad M, Lindholm J, Martling A, Blomqvist L. Retrospective measurement of different size parameters of non-radiated rectal cancer on MR images and pathology slides and their comparison. *Eur Radiol* 2003; 13:2271–2277
27. Chau I, Brown G, Cunningham D, et al. Neoadjuvant capecitabine and oxaliplatin followed by synchronous chemoradiation and total mesorectal excision in magnetic resonance imaging–defined poor-risk rectal cancer. *J Clin Oncol* 2006; 24:668–674
28. Therasse P, Arbuck SG, Eisenhauer EA, et al. New guidelines to evaluate the response to treatment in solid tumors. European Organization for Research and Treatment of Cancer, National Cancer Institute of the United States, National Cancer Institute of Canada. *J Natl Cancer Inst* 2000; 92:205–216
29. Dewdney A, Cunningham D, Tabernero B, et al. EXPERT-C: a randomized phase II European multicenter trial of neoadjuvant chemotherapy (capecitabine/oxaliplatin) and chemoradiation (CRT) with or without cetuximab followed by total mesorectal excision (TME) in patients with MRI-defined high-risk rectal cancer (abstr). *J Clin Oncol* 2011; 29(suppl 4):abstract 360
30. Patel UB, Brown G, Rutten H, et al. Comparison of magnetic resonance imaging and histopathological response to chemoradiotherapy in locally advanced rectal cancer. *Ann Surg Oncol* 2012 Apr 24 [Epub ahead of print]
31. Dworak O, Keilholz L, Hoffmann A. Pathological features of rectal cancer after preoperative radiochemotherapy. *Int J Colorectal Dis* 1997; 12:19–23
32. Mandard AM, Dalibard F, Mandard JC, et al. Pathologic assessment of tumor regression after preoperative chemoradiotherapy of esophageal carcinoma: clinicopathologic correlations. *Cancer* 1994; 73:2680–2686
33. Rödel C, Martus P, Papadoupolos T, et al. Prognostic significance of tumor regression after preoperative chemoradiotherapy for rectal cancer. *J Clin Oncol* 2005; 23:8688–8696
34. Taylor FG, Swift RI, Blomqvist L, Brown G. A systematic approach to the interpretation of preoperative staging MRI for rectal cancer. *AJR* 2008; 191:1827–1835
35. Hermanek P, Hutter R, Sobin LH, et al., eds. *TNM supplement 1993: a commentary on uniform use*. Berlin, Germany: Springer-Verlag, 1993
36. Taylor FG, Quirke P, Heald RJ, et al. One millimetre is the safe cut-off for magnetic resonance imaging prediction of surgical margin status in rectal cancer. *Br J Surg* 2011; 98:872–879
37. Shihab OC, Taylor F, Salerno G, et al. MRI predictive factors for long-term outcomes of low rectal tumours. *Ann Surg Oncol* 2011; 18:3278–3284
38. Shihab OC, How P, West N, et al. Can a novel MRI staging system for low rectal cancer aid surgical planning? *Dis Colon Rectum* 2011; 54:1260–1264
39. Salerno GV, Daniels IR, Moran BJ, Heald RJ, Thomas K, Brown G. Magnetic resonance imaging prediction of an involved surgical resection margin in low rectal cancer. *Dis Colon Rectum* 2009; 52:632–639
40. Marone P, de Bellis M, Avallone A, et al. Accuracy of endoscopic ultrasound in staging and restaging patients with locally advanced rectal cancer undergoing neoadjuvant chemoradiation. *Clin Res Hepatol Gastroenterol* 2011; 35:666–670
41. Rau B, Hunerbein M, Barth C, et al. Accuracy of endorectal ultrasound after preoperative radiochemotherapy in locally advanced rectal cancer. *Surg Endosc* 1999; 13:980–984
42. Gavioli M, Bagni A, Piccagli I, Fundaro S, Natalini G. Usefulness of endorectal ultrasound after preoperative radiotherapy in rectal cancer: comparison between sonographic and histopathologic changes. *Dis Colon Rectum* 2000; 43:1075–1083
43. Koh DM, Chau I, Tait D, Wotherspoon A, Cunningham D, Brown G. Evaluating mesorectal lymph nodes in rectal cancer before and after neoadjuvant chemoradiation using thin-section T2-weighted magnetic resonance imaging. *Int J Radiat Oncol Biol Phys* 2008; 71:456–461
44. Shirouzu K, Isomoto H, Kakegawa T, Morimatsu M. A prospective clinicopathologic study of venous invasion in colorectal cancer. *Am J Surg* 1991; 162:216–222
45. Saclarides TJ, Bhattacharyya AK, Britton-Kuzel C, Szeluga D, Economou SG. Predicting lymph node metastases in rectal cancer. *Dis Colon Rectum* 1994; 37:52–57
46. Talbot IC, Ritchie S, Leighton MH, Hughes AO, Bussey HJ, Morson BC. The clinical significance of invasion of veins by rectal cancer. *Br J Surg* 1980; 67:439–442
47. Smith NJ, Shihab O, Arnaout A, Swift RI, Brown G. MRI for detection of extramural vascular invasion in rectal cancer. *AJR* 2008; 191:1517–1522
48. Smith NJ, Barbachano Y, Norman AR, Swift RI, Abulafi AM, Brown G. Prognostic significance of magnetic resonance imaging–detected extramural vascular invasion in rectal cancer. *Br J Surg* 2008; 95:229–236
49. Smith N, Brown G. Preoperative staging of rectal cancer. *Acta Oncol* 2008; 47:20–31
50. Burton S, Brown G, Daniels I, et al. MRI identified prognostic features of tumors in distal sigmoid, rectosigmoid, and upper rectum: treatment with radiotherapy and chemotherapy. *Int J Radiat Oncol Biol Phys* 2006; 65:445–451
51. Dighe S, Swift I, Magill L, et al. Accuracy of radiological staging in identifying high-risk colon cancer patients suitable for neoadjuvant chemotherapy: a multicentre experience. *Colorectal Dis* 2012; 14:438–444
52. Brown G, Daniels IR, Richardson C, Revell P, Peppercorn D, Bourne M. Techniques and troubleshooting in high spatial resolution thin slice MRI for rectal cancer. *Br J Radiol* 2005; 78:245–251